Advanced Pharmaceutical Bulletin

Accepted Manuscript (unedited)

The manuscript will undergo copyediting, typesetting, and review of the resulting proof before it is published in its final form.

Research Article

How to cite this article:
Valizadeh A, Rahmati-Yamchi M, Ali Hemmati A, Ebrahimnezhad M, Yousefzadeh A, Molavand M, Yousefi B. Targeting p53/p21 Signaling: Linarin as a Novel Modulator of 5-FU Sensitization in Colorectal Cancer. Advanced Pharmaceutical Bulletin, doi: 10.34172/apb.47354

Targeting p53/p21 Signaling: Linarin as a Novel Modulator of 5-FU Sensitization in Colorectal Cancer

Amir Valizadeh[a,b], Mohammad Rahmati-Yamchi[b], Alireza Ali Hemmati[c], Mohammad Ebrahimnezhad[a], Ali Yousefzadeh[a], Mehran Molavand[a,b], Bahman Yousefi[b*]

[a] Student Research Committee, Tabriz University of Medical Sciences, Tabriz, Iran
[b] Department of Clinical Biochemistry and Laboratory Medicine, Faculty of Medicine, Tabriz University of Medical Sciences, Tabriz, Iran
[c] Department of Anatomical Sciences, Faculty of Medicine, Tabriz University of Medical Sciences, Tabriz, Iran

ARTICLE INFO

Keywords:
Linarin,
5-Fluorouracil,
Colorectal cancer,
p53 pathway,
Combination therapy

Article History:
Submitted: April 10, 2026
Revised: June 10, 2026
Accepted: July 20, 2026
ePublished: August 09, 2026

ABSTRACT

Purpose: We assessed linarin, a plant-derived flavone glycoside, for its ability to overcome intrinsic 5-fluorouracil (5-FU) resistance by reinstating p53/p21-mediated tumor suppression in colorectal cancer (CRC) cell models, and we explicitly present these findings as a mechanistic proof of concept within a defined in vitro scope.
Methods: Cell viability was measured using the MTT assay; synergy was assessed using the combination index (CI) with isobologram validation; and programmed cell death was evaluated by internucleosomal DNA fragmentation ELISA and Western blot analysis of caspase-dependent markers. Underlying pathways were probed by immunoblotting, quantitative RT-PCR, and targeted siRNA-mediated knockdown of p53 and p21, complemented by pharmacological inhibition with pifithrin-α and UC2288.
Results: Linarin induced concentration-dependent cell killing in CRC lines, yielding IC_{50} values of 122.8–210.2 μM at 48 hours, alongside selective sparing of normal colon cells (NCM460; selectivity index approximately 2.0–3.3-fold). The p53 status-dependent sensitivity gradient (HCT116 wild-type < SW480 mutant < HCT116 $p53^{-/-}$) provided initial evidence of p53-dependent cytotoxicity. Dual therapy with 5-FU yielded robust synergy (CI 0.52–0.88) in p53-proficient lines, with near-additive effects in p53-null cells (CI 0.77), and notably reduced the 5-FU IC_{50} in intrinsically resistant LoVo cells from 19.0 μM to 5.7 μM. Linarin promoted p53 stabilization and Ser15/Ser20 phosphorylation, elevated p21 mRNA levels to 5.4-fold the control level, and suppressed MDM2 mRNA levels to 0.42-fold the control level. This was accompanied by caspase-dependent cell death and amplified DNA damage signaling (elevated γ-H2AX). Functional validation via siRNA knockdown and pharmacological inhibition confirmed the centrality of the p53/p21 pathway in linarin's sensitizing action in p53-competent cells.
Conclusion: As a mechanistic proof-of-concept, linarin demonstrates the capacity to potentiate 5-FU cytotoxicity by reactivating the p53/p21 pathway in CRC models harboring functional p53. Future investigations should prioritize models of acquired resistance and formulation optimization to advance these findings toward preclinical translation.

***Corresponding Author**
Bahman Yousefi, Email: bahmanusefi@gmail.com, ORCID: 0000-0002-4220-1527

Introduction

Colorectal cancer (CRC) remains the third most commonly diagnosed cancer worldwide and the second leading cause of cancer-related mortality, accounting for approximately 935,000 deaths annually. Despite significant advances in surgical techniques, targeted therapies, and immunotherapy, the five-year survival rate for metastatic CRC remains disappointingly low at less than 15%.[1,2] The primary therapeutic challenge in CRC management is the development of chemoresistance, particularly to 5-fluorouracil (5-FU), which has served as the backbone of CRC chemotherapy for over six decades.[3,4]

5-FU exerts its anticancer effects through multiple mechanisms, including inhibition of thymidylate synthase (TS), incorporation into RNA and DNA, and induction of DNA damage-mediated apoptosis. However, the clinical efficacy of 5-FU is frequently compromised by both intrinsic and acquired resistance mechanisms. These include alterations in drug metabolism enzymes such as dihydropyrimidine dehydrogenase (DPD) and TS, enhanced DNA repair capacity, dysregulation of apoptotic pathways, and, most critically, inactivation of the p53 tumor suppressor pathway.[5,6] The p53 protein, often referred to as the "guardian of the genome," plays a pivotal role in maintaining cellular homeostasis by coordinating DNA damage responses, cell cycle checkpoints, and apoptotic programs in response to various cellular stresses.

The p53 pathway is frequently disrupted in CRC, with mutations occurring in approximately 40–50% of cases. Wild-type p53 functions as a sequence-specific transcription factor that regulates the expression of numerous target genes involved in cell cycle arrest, DNA repair, senescence, and apoptosis.[7] Upon activation by cellular stress signals, p53 undergoes post-translational modifications, including phosphorylation at serine residues 15 and 20, which stabilize the protein and enhance its transcriptional activity. One of the most critical p53 target genes is CDKN1A, also known as p21(WAF1/CIP1), which encodes the cyclin-dependent kinase inhibitor p21. The p53–p21 axis serves as a crucial checkpoint mechanism that allows cells to either repair DNA damage or undergo apoptosis when damage is irreparable.[8]

Natural compounds have emerged as valuable sources for developing novel anticancer therapeutics, with many demonstrating the ability to modulate key cellular pathways involved in tumorigenesis and chemoresistance.[9] Among structurally diverse flavonoids investigated as chemosensitizers — including quercetin, apigenin, and acacetin — flavone glycosides represent an underexplored subclass with distinct pharmacological profiles attributable to their sugar moieties. Linarin (acacetin-7-O-β-D-glucopyranoside) is a naturally occurring flavone glycoside found in various medicinal plants, including Chrysanthemum morifolium, Buddleja officinalis, and Cirsium japonicum.[10] Structurally, linarin consists of an acacetin aglycone linked to a glucose moiety, which may influence its bioavailability and cellular uptake. Previous studies have reported various biological activities of linarin, including hepatoprotective, nephroprotective, anti-inflammatory, and antioxidant effects.[11] However, its potential anticancer properties, particularly in CRC, remain largely unexplored.

Our specific objectives were to: (1) evaluate the cytotoxic effects of linarin across a panel of CRC cell lines with different p53 status; (2) assess potential synergistic interactions between linarin and 5-FU, with isobologram validation; (3) elucidate the molecular mechanisms underlying linarin's anticancer activity, with a focus on the p53/p21 pathway; (4) determine the functional consequences of p53 pathway modulation, including target gene expression and caspase-dependent cell death; and (5) establish the causal relationship between p53 pathway

activation and linarin-mediated sensitization to 5-FU through loss-of-function studies. These objectives are explicitly framed as mechanistic proof-of-concept aims within an in vitro experimental system, with full acknowledgment that acquired resistance modeling, upstream kinase characterization, flow cytometric validation, and in vivo pharmacokinetic studies represent essential components of the next investigative phase.

Materials and Methods

Cell lines and culture conditions

Human CRC cell lines HCT116 (p53 wild-type), HCT116 $p53^{-/-}$ (p53-knockout), SW480 (p53 mutant, R273H/P309S gain-of-function), and LoVo (intrinsically resistant to 5-FU, with functional p53 impairment documented in the literature)[12] were obtained from the American Type Culture Collection (ATCC, Manassas, VA, USA). Normal human colonic epithelial cells (NCM460) were used as the closest available immortalized surrogate for normal colonic epithelium; we acknowledge that NCM460 cells are immortalized and may not fully recapitulate the drug sensitivity of primary intestinal epithelial cells, which represents a limitation of the current selectivity assessment. All cell lines were authenticated by short tandem repeat (STR) profiling and tested negative for mycoplasma contamination using the MycoAlert Mycoplasma Detection Kit (Lonza, Basel, Switzerland).

Cells were maintained in RPMI-1640 medium (Gibco, Thermo Fisher Scientific, Waltham, MA, USA) supplemented with 10% fetal bovine serum (FBS, Sigma-Aldrich, St. Louis, MO, USA), 100 U/mL penicillin, and 100 μg/mL streptomycin at 37°C in a humidified atmosphere containing 5% CO_2. Cells were subcultured every 2–3 days and used for no more than 15 passages. The LoVo cell line was employed in this study as a model of intrinsic, rather than acquired, 5-FU resistance. The generation of stable acquired 5-FU-resistant sublines through chronic drug exposure, with full characterization of resistance markers including thymidylate synthase upregulation, DPD overexpression, and ABC transporter profiling, was not feasible within the resource constraints of the current Ph.D.-funded project. We explicitly acknowledge this as a defined scope limitation and designate the development and pharmacological evaluation of acquired 5-FU-resistant CRC sublines as the primary experimental priority in the subsequent phase of this research program. The 5-FU intrinsic resistance profile of LoVo cells was verified in our laboratory at study initiation and confirmed to be stable across the passage range used (passages 5–12).

Chemical reagents and antibodies

Linarin (purity >98%) was purchased from Sigma-Aldrich and dissolved in dimethyl sulfoxide (DMSO) to prepare a 100 mM stock solution. All experiments included vehicle controls with DMSO concentrations matched to those of the treatment groups, with final DMSO concentrations never exceeding 0.1% (v/v) to avoid solvent-mediated cytotoxicity. Preliminary experiments confirmed that DMSO at ≤0.1% did not affect cell viability or protein expression. 5-FU was obtained from Sigma-Aldrich and dissolved in sterile water. Pifithrin-α (p53 inhibitor) and UC2288 (p21 inhibitor) were purchased from Selleck Chemicals (Houston, TX, USA).

Primary antibodies against p53 (DO-1), p21 (F-5), p-p53 (Ser15), p-p53 (Ser20), MDM2 (SMP14), caspase-3 (Asp175), cleaved PARP (Asp214), γ-H2AX (Ser139), and GAPDH were purchased from Santa Cruz Biotechnology (Dallas, TX, USA) or Cell Signaling Technology (Danvers, MA, USA). Secondary antibodies

conjugated with horseradish peroxidase (HRP) were obtained from Jackson ImmunoResearch (West Grove, PA, USA).

Cell viability and proliferation assays

Cell viability was assessed using the MTT (3-(4,5-dimethylthiazol-2-yl)-2,5-diphenyltetrazolium bromide) assay. Cells were seeded in 96-well plates at a density of 5×10^3 cells/well and treated with various concentrations of linarin (0–1000 μM), 5-FU (0–64 μM), or combination treatments for 48 hours. MTT solution (5 mg/mL) was added to each well, and the mixture was incubated for 4 hours at 37°C. The formazan crystals were dissolved in DMSO, and absorbance was measured at 570 nm using a microplate reader (BioTek, Winooski, VT, USA).

The combination index (CI) was calculated using CompuSyn software (ComboSyn Inc., Paramus, NJ, USA) based on the Chou–Talalay median-effect method.[13] Combination treatments were performed using a constant-ratio variation with linarin held at 50 μM (approximately IC_{20}–IC_{30} across cell lines) and varying concentrations of 5-FU (0–64 μM). Isobologram plots were generated for each cell line using CompuSyn to visually confirm synergistic interactions. CI < 1 indicates synergism, CI = 1 indicates additivity, and CI > 1 indicates antagonism.

Detection of apoptosis using cytoplasmic histone-associated DNA fragments

The Cell Death Detection ELISA Plus Kit (Roche) was used to assess caspase-dependent programmed cell death induction according to the manufacturer's instructions. This assay measures internucleosomal DNA fragmentation, a biochemically specific marker of apoptotic cell death that is mechanistically distinct from the non-specific DNA release associated with necrotic cell death. Briefly, cells were seeded in 96-well plates and treated with the respective compounds for 48 hours. After treatment, cells were lysed, and cytoplasmic fractions were collected. Samples were then treated with an immunoreagent containing peroxidase-conjugated anti-DNA and biotin-labeled anti-histone antibodies. Absorbance was determined at 405 nm using a BioTek microplate reader. Western blot analysis of cleaved caspase-3 and cleaved PARP provided orthogonal biochemical confirmation of caspase-dependent apoptotic execution. We acknowledge that these assays provide convergent biochemical evidence consistent with apoptosis. Still, that definitive quantification of apoptotic and necrotic populations by Annexin V/PI flow cytometry — the gold standard for this purpose — was not performed in the current study due to constraints on instrument availability. Flow cytometric apoptosis quantification is explicitly designated as a high-priority validation experiment in the follow-up investigation. We further acknowledge that non-apoptotic cell death mechanisms, including necroptosis, ferroptosis, and autophagic cell death, have not been excluded and will require assessment in future studies.

Western blot analysis

Whole cell lysates were prepared using RIPA buffer containing protease and phosphatase inhibitors (Thermo Fisher Scientific). Protein concentrations were determined using the Bradford assay (Bio-Rad, Hercules, CA, USA). Equal amounts of protein (30–50 μg) were separated by SDS-PAGE and transferred to PVDF membranes (Millipore, Burlington, MA, USA). Membranes were blocked with 5% non-fat milk in TBST for 1 hour, then incubated with primary antibodies overnight at 4°C. This was followed by incubation with HRP-conjugated secondary antibodies for 1 hour at room temperature. Protein bands were visualized using enhanced chemiluminescence (ECL) reagent (GE Healthcare, Chicago, IL, USA) and quantified using ImageJ software

(NIH, Bethesda, MD, USA). Band intensities were normalized to the GAPDH loading control for each lane. Raw and processed Western blot images are provided in Supplementary File 1 (Figure S1).

Quantitative Real-Time PCR (qRT-PCR)

Total RNA was extracted using TRIzol reagent (Invitrogen, Carlsbad, CA, USA) and reverse transcribed using the High-Capacity cDNA Reverse Transcription Kit (Applied Biosystems, Foster City, CA, USA). qRT-PCR was performed using SYBR Green Master Mix (Applied Biosystems) on a StepOnePlus Real-Time PCR System. Primer sequences, amplicon sizes, annealing temperatures, and corresponding NCBI RefSeq accession numbers are presented in Supplementary Table S1.

Gene expression levels were normalized to GAPDH and calculated using the $2^{-\Delta\Delta C_t}$ method. Before experimental analysis, primer efficiency was validated for all primer pairs using five-point standard curves (10-fold serial dilutions of pooled cDNA), with all primers demonstrating amplification efficiencies between 90–110% and R^2 values >0.98. GAPDH was selected as the reference gene after validation studies confirmed its stable expression across all experimental conditions (Ct standard deviation <0.5 across treatment groups). Melt curve analysis was performed for all amplifications to confirm product specificity.

RNA interference

Small interfering RNAs (siRNAs) targeting p53 (si-p53), p21 (si-p21), or a negative control (si-NC) were purchased from GenePharma (Shanghai, China). Cells were transfected with siRNA (50 nM) using Lipofectamine RNAiMAX (Invitrogen) according to the manufacturer's protocol. Knockdown efficiency was verified by Western blot and qRT-PCR after 48 to 72 hours.

Statistical analysis

All experiments were performed at least three times independently with triplicate samples (n = 3 independent biological replicates, each with technical triplicates). Data are presented as mean ± standard deviation (SD). Before parametric analysis, data normality was assessed using the Shapiro–Wilk test, and homogeneity of variance was confirmed using Levene's test. Statistical analysis was performed using GraphPad Prism 9.0 software (GraphPad Software, San Diego, CA, USA). Differences between groups were analyzed using a Student's t-test (for two groups) or a one-way ANOVA followed by Tukey's post hoc test (for multiple groups), with ANOVA assumptions confirmed. A p-value <0.05 was considered statistically significant. The sample size of n = 3 independent biological replicates is consistent with standard practice for initial in vitro mechanistic proof-of-concept studies and was sufficient to detect the effect sizes observed (>2-fold differences); formal a priori power analysis will be incorporated in future in vivo study designs.

Results

Linarin exhibits dose-dependent cytotoxicity in colorectal cancer cells with p53 status-dependent sensitivity

To evaluate the anticancer potential of linarin, we first examined its effects on cell viability in various CRC cell lines. MTT assays showed that linarin treatment reduced cell viability in a dose-dependent manner across all tested CRC cell lines (Figure 1A). The IC_{50} values of linarin at 48 hours were 122.8 ± 8.8 μM for HCT116, 200.7 ± 10.1

μM for SW480, and 210.2 ± 11.1 μM for LoVo cells, while normal colonic epithelial cells (NCM460) showed significantly higher resistance with an IC_{50} of 410.7 ± 22.4 μM ($p<0.001$ vs. all CRC lines; selectivity index 2.0–3.3). Similarly, 5-FU produced dose-dependent effects across cell lines (Figure 1B).

The sensitivity profile across our cell panel followed a p53 status-dependent gradient: HCT116 p53-null cells demonstrated significantly reduced sensitivity to linarin compared to their wild-type counterparts (IC_{50}: 189.7 ± 9.2 vs. 122.8 ± 8.8 μM, $p<0.01$), and SW480 cells harboring gain-of-function mutant p53 (R273H/P309S) showed intermediate sensitivity (IC_{50}: 200.7 ± 10.1 μM, $p<0.05$ vs. HCT116 wild-type). This gradient — wild-type < mutant < null < normal — is consistent with p53-dependent modulation of sensitivity, while the residual cytotoxicity in p53-null cells indicates that p53-independent pathways also contribute at the concentrations tested. We acknowledge that the IC_{50} values reported here substantially exceed estimated achievable plasma concentrations of unmodified linarin following oral administration, and that this represents a significant pharmacological consideration. The translational implications of these concentration requirements are addressed in detail in the Discussion section.

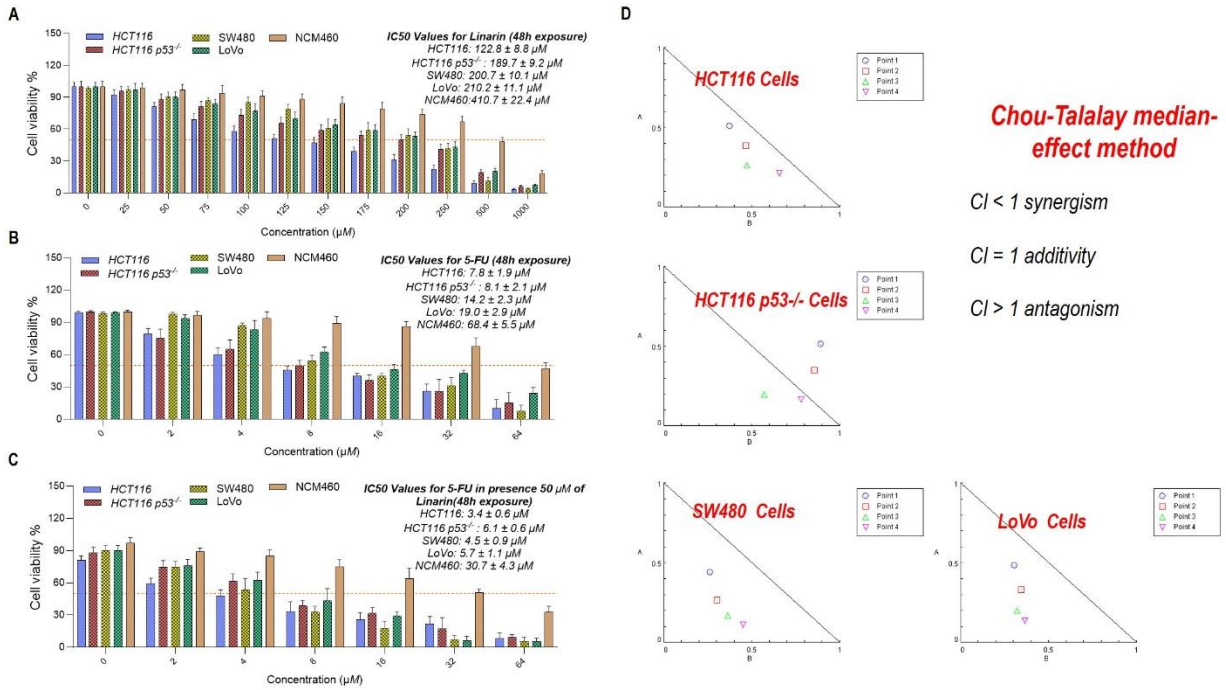

Figure 1. Linarin exhibits cytotoxic effects and synergizes with 5-FU in colorectal cancer cells. Dose-response bars showing the cytotoxic effects of (A) linarin and (B) 5-FU on various colorectal cancer cell lines and normal colonic epithelial cells (NCM460) after 48-hour treatment. (C) Combination therapy significantly reduces the 5-FU IC_{50} value in LoVo cells from 19.0 ± 2.9 μM to 5.7 ± 1.1 μM. (D) Isobologram analysis confirming synergistic interactions for HCT116 and LoVo cells, with data points plotting below the line of additivity. Data points represent mean ± SD from three independent biological replicates (n = 3), each performed in technical triplicate. **5-FU:** 5-fluorouracil; **SD:** standard deviation; **IC_{50}:** half maximal inhibitory concentration.

Linarin synergistically enhances 5-fluorouracil sensitivity in p53-competent cells

Combination treatment with linarin (50 μM) and 5-FU at various concentrations resulted in synergistic cytotoxic effects across all p53 wild-type cell lines, with CI values ranging from 0.52 to 0.88 (Table 1). The most pronounced synergistic effect was observed in the intrinsically chemoresistant LoVo cells, where the combination

treatment reduced the 5-FU IC_{50} from approximately 19 µM to approximately 5 µM, representing a 70% reduction (Figure 1C). We note that LoVo cells represent a model of intrinsic, rather than acquired, 5-FU resistance, and that the generalizability of these findings to acquired resistance contexts will require evaluation in dedicated acquired-resistant sublines in future studies. Importantly, this synergistic effect was substantially reduced in HCT116 p53-null cells (CI = 0.77), approaching additivity, confirming that synergism is preferentially observed in p53-competent cells. SW480 cells showed synergy (CI = 0.70), intermediate between p53 wild-type and null lines, consistent with the partial p53-dependent mechanism hypothesis. Isobologram analysis confirmed that data points for HCT116 and LoVo combinations fell consistently below the line of additivity, providing visual confirmation of synergy (Figure 1D; Supplementary File 1, Figure S2).

Selectivity index = NCM460 IC_{50} / CRC line IC_{50}. The corrected selectivity range for the abstract is ~2.0–3.3.

Table 1. Combination index analysis of linarin and 5-FU treatment.

Cell Line	Linarin (µM)	5-FU (µM)	Combination Index (CI)	Effect
HCT116	50	2	0.88 ± 0.10	Synergistic
HCT116	50	4	0.85 ± 0.08	Synergistic
HCT116	50	8	0.73 ± 0.09	Synergistic
HCT116 $p53^{-/-}$	50	8	0.77 ± 0.11	Synergistic
SW480	50	2	0.70 ± 0.07	Synergistic
SW480	50	4	0.57 ± 0.06	Synergistic
SW480	50	8	0.53 ± 0.07	Synergistic
LoVo	50	2	0.79 ± 0.09	Synergistic
LoVo	50	4	0.67 ± 0.08	Synergistic
LoVo	50	8	0.52 ± 0.05	Synergistic

Note: 5-FU: 5-fluorouracil; **µM:** micromolar; **CI:** combination index; **$p53^{-/-}$:** p53-null. CI values calculated using CompuSyn software based on the Chou–Talalay median-effect method; CI < 1 indicates synergism, CI = 1 indicates additivity, and CI > 1 indicates antagonism. Data represent mean ± SD from three independent experiments.

Linarin induces caspase-dependent programmed cell death

To investigate the mechanism underlying linarin-induced cytotoxicity, we analyzed programmed cell death markers following treatment. Linarin treatment (50 µM, 48 hours) significantly increased apoptotic cell death in HCT116 cells from 14.02 ± 2.8% to 45.9 ± 5.2% ($p<0.001$), as determined by internucleosomal DNA fragmentation ELISA in the combination treatment group (Figure 2A). Western blot analysis revealed increased expression of cleaved caspase-3 and cleaved PARP, providing orthogonal biochemical confirmation of caspase-dependent programmed cell death (Figure 2B). The effect was attenuated in HCT116 p53-null cells and intermediate in LoVo cells, consistent with the p53-dependent pattern observed in viability assays. These convergent findings from two independent biochemical assays — internucleosomal DNA fragmentation ELISA and caspase/PARP Western blot analysis — provide evidence consistent with caspase-dependent apoptosis. We explicitly acknowledge that Annexin V/PI flow cytometry, which represents the definitive method for distinguishing apoptotic from necrotic and viable populations, was not performed in the current study, and that this constitutes a defined limitation. Flow cytometric apoptosis quantification is prioritized as an essential

validation experiment in the next phase of investigation. We further acknowledge that necroptosis, ferroptosis, and autophagic cell death have not been excluded.

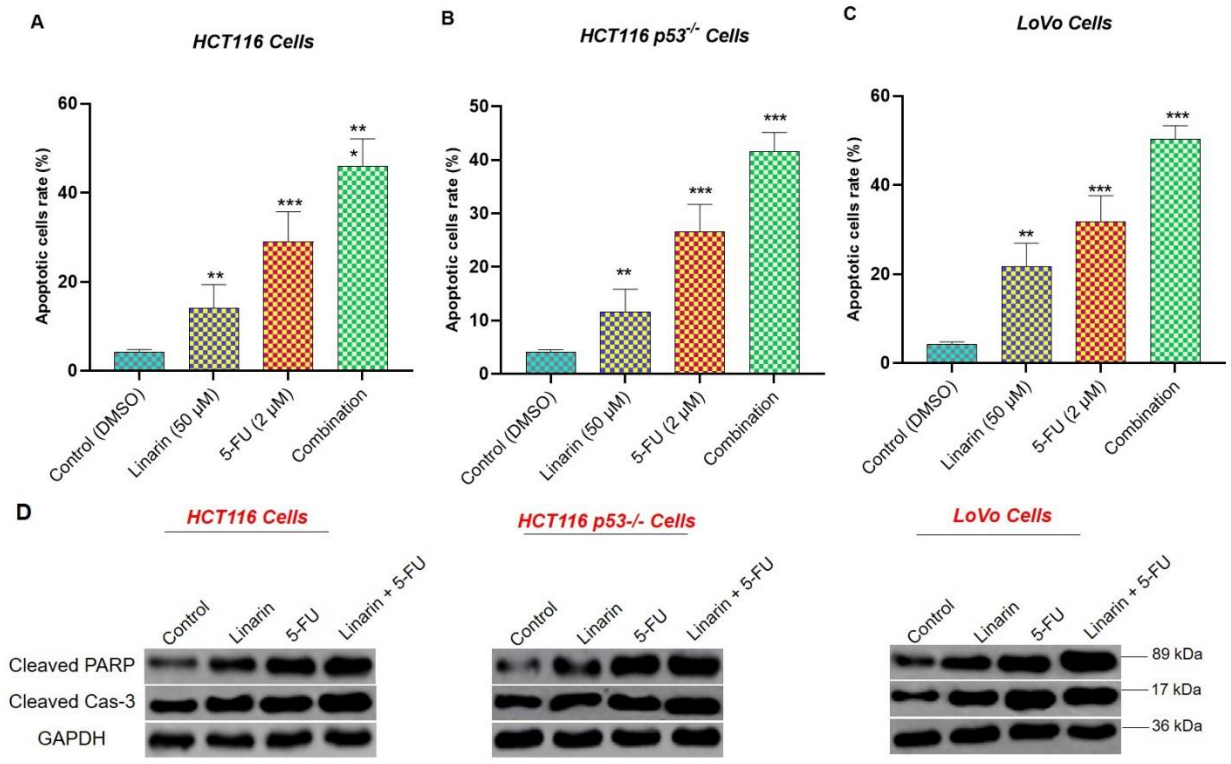

Figure 2. Linarin induces caspase-dependent programmed cell death. (A) Bar graph showing percentage of apoptotic cells determined by internucleosomal DNA fragmentation ELISA after treatment with linarin (50 μM), 5-FU (2 μM), and their combination for 48 hours in HCT116, HCT116 $p53^{-/-}$, and LoVo cells. (B) Western blot analysis of apoptosis-related proteins, including cleaved caspase-3 and cleaved PARP. GAPDH serves as a loading control. Data points represent mean ± SD from three independent biological replicates (n = 3), each performed in technical triplicate. **p<0.01, ***p<0.001 vs. control. **5-FU:** 5-fluorouracil; **SD:** Standard deviation; **ELISA:** Enzyme-Linked Immunosorbent Assay; **PARP:** Poly(ADP-ribose) polymerase; **GAPDH:** Glyceraldehyde 3-phosphate dehydrogenase; **μM:** Micromolar.

Linarin promotes p53 stabilization and transcriptional activation

qRT-PCR analysis revealed significant modulation of p53 pathway target genes following linarin treatment (50 μM, 48 hours). In HCT116 cells, p53 mRNA levels increased 2.8 ± 0.3-fold ($p<0.01$ vs. control), p21 mRNA levels increased 5.4 ± 0.6-fold ($p<0.001$), and MDM2 mRNA levels decreased to 0.42 ± 0.08-fold of control values ($p<0.01$). Similar patterns were observed in LoVo cells, with p53 increasing 2.3 ± 0.4-fold ($p<0.05$), p21 increasing 4.7 ± 0.5-fold ($p<0.001$), and MDM2 decreasing to 0.38 ± 0.06-fold ($p<0.01$; Figure 3A). Western blot analysis confirmed p53 protein stabilization and phosphorylation at Ser15 and Ser20, consistent with enhanced post-translational stabilization, alongside MDM2 protein downregulation (Figure 3B). No changes in p53 mRNA or protein were detected in HCT116 p53-null cells, confirming assay specificity.

The parallel reduction of MDM2 at both mRNA and protein levels is consistent with transcriptional repression as the primary mechanism of MDM2 suppression. However, we acknowledge that the precise upstream mechanism by which linarin promotes Ser15 and Ser20 phosphorylation remains to be fully characterized. Specifically, determination of whether linarin activates ATM or ATR kinases — the principal upstream mediators

of p53 stabilization in response to DNA damage — was not performed in the current study. Similarly, p53-responsive luciferase transcriptional reporter assays, which would provide direct quantitative evidence of enhanced p53 transcriptional activity, and co-immunoprecipitation-based assessment of MDM2–p53 physical interaction, were not conducted. These mechanistic studies require dedicated reporter constructs, kinase activity assay platforms, and immunoprecipitation-grade reagents that were not available within the resource constraints of the current Ph.D.-funded project. We designate ATM/ATR activation studies, p53 transcriptional reporter assays, and MDM2–p53 co-immunoprecipitation analysis as the highest-priority mechanistic experiments in the next phase of this investigation. The current data are therefore presented as evidence consistent with p53 stabilization through post-translational modification and transcriptional suppression of MDM2, rather than as a fully delineated upstream mechanistic characterization.

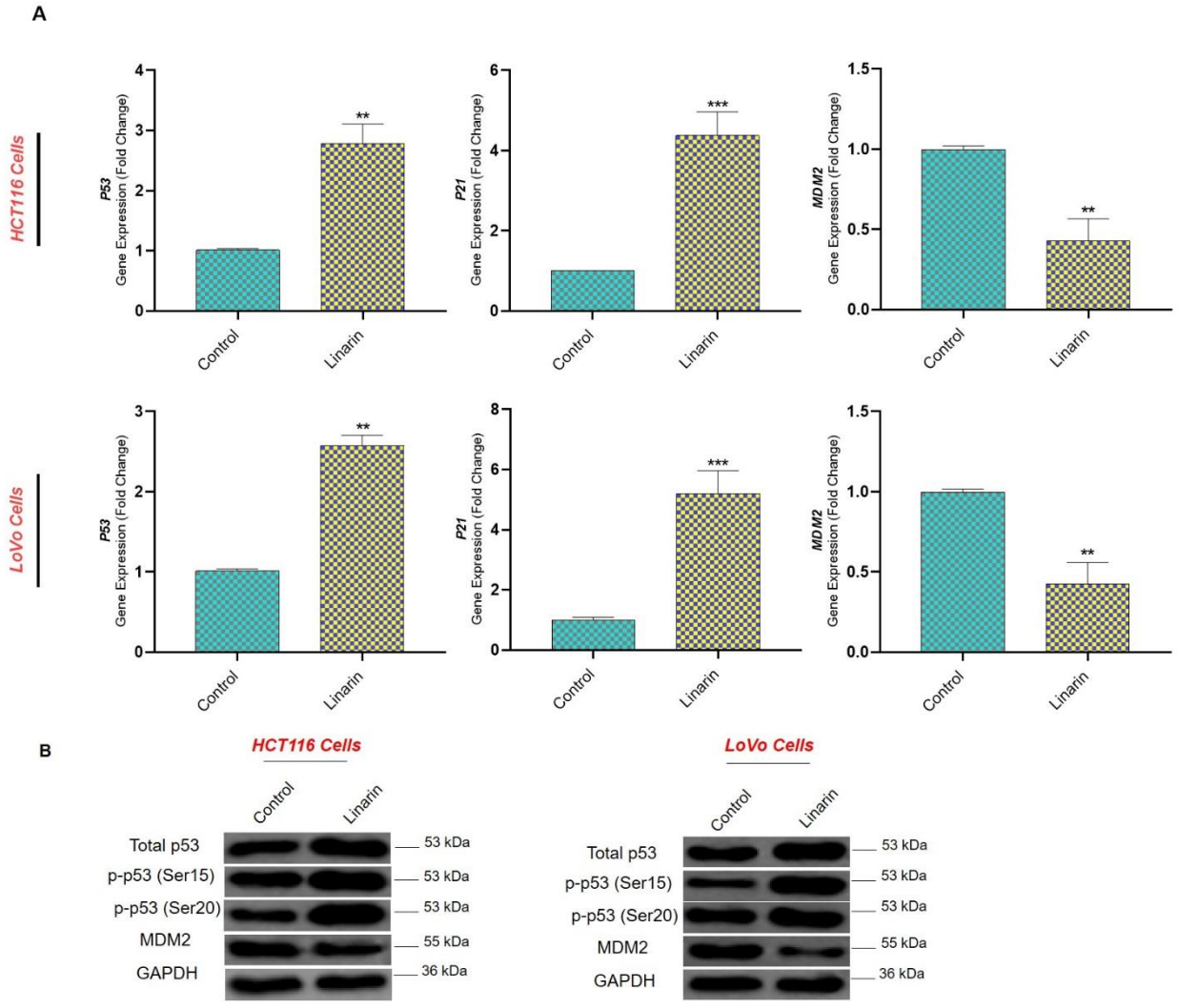

Figure 3. Linarin activates p53 and enhances its transcriptional activity. (A) mRNA expression levels of p53, p21, and MDM2 in HCT116 and LoVo cells treated with linarin (50 μM) for 48 hours, normalized to GAPDH ($2^{-\Delta\Delta C_t}$ method). (B) Western blot analysis showing increases in total p53 and phospho-p53 (Ser15 and Ser20), along with decreased MDM2 expression, in HCT116 and LoVo cells after 48 hours of linarin treatment. Band intensities were normalized to GAPDH and quantified by ImageJ. Data points represent mean ± SD from three independent biological replicates (n = 3), each performed in technical triplicate. *p<0.05, **p<0.01, ***p<0.001 vs. control. **5-FU:** 5-fluorouracil; **SD:** Standard deviation; **MDM2:** Mouse double minute 2 homolog**.**

The p53/p21 pathway is essential for linarin-mediated sensitization

To establish the causal role of the p53/p21 axis in linarin's effects, we employed loss-of-function approaches. Knockdown of p53 using siRNA significantly attenuated linarin-induced cytotoxicity, resulting in reduced cell death in HCT116 and LoVo cells ($p<0.05$ vs. si-NC controls; Figure 4A). Knockdown efficiency was confirmed to exceed 80% at both mRNA and protein levels. Similarly, p21 knockdown partially rescued cells from linarin-induced programmed cell death, demonstrating the functional importance of p21 downstream of p53 activation. Pharmacological inhibition of p53 with pifithrin-α (30 μM) or of p21 with UC2288 (20 μM) significantly reduced both the cytotoxic effects of linarin alone and the synergistic effects observed in combination with 5-FU (Figure 4B; all $p<0.01$ vs. vehicle control). These results confirm, through two independent loss-of-function strategies, that the p53/p21 pathway is a critical mediator of linarin's sensitizing effects in p53-competent CRC cells. We note that these functional validation data constitute the most direct evidence available in the current dataset for the causal role of the p53/p21 axis and are particularly important given the incomplete upstream mechanistic characterization discussed above.

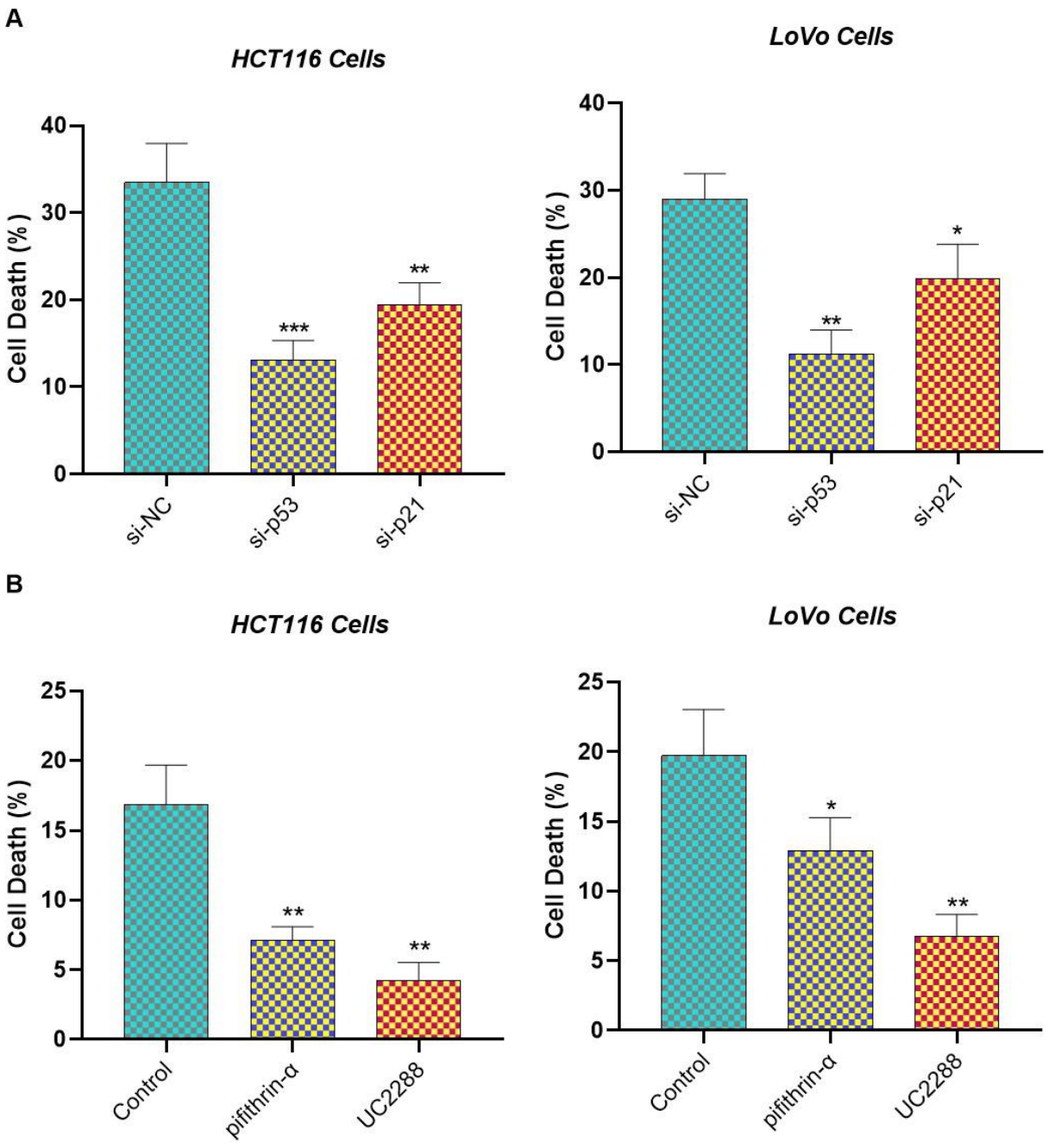

Figure 4. The p53/p21 pathway is essential for linarin-mediated sensitization. (A) Effect of p53 and p21 siRNA knockdown on linarin-induced cytotoxicity in HCT116 and LoVo cells. The bar graph shows the percentage of cell death after 48 hours of treatment with 50 μM linarin following siRNA transfection. (B) Impact of pharmacological inhibitors (pifithrin-α for p53; UC2288 for p21) on the synergistic effects of the linarin and 5-FU combination. Data represent mean ± SD from three independent biological replicates (n = 3), each with technical triplicates. *p<0.05, **p<0.01 vs. si-NC or vehicle control. **5-FU:** 5-fluorouracil; **SD:** Standard deviation; **MDM2:** Mouse double minute 2 homolog; **μM:** Micromolar; **siRNA:** Small interfering RNA; **si-NC:** Negative control siRNA.

Linarin induces DNA damage signaling

Western blot analysis of γ-H2AX (Ser139), an established marker of DNA double-strand break signaling, demonstrated significant induction following linarin treatment in both HCT116 and LoVo cells. γ-H2AX band intensity increased 3.2 ± 0.4-fold in HCT116 and 2.9 ± 0.5-fold in LoVo cells following linarin treatment (50 μM, 48 hours) relative to DMSO control ($p<0.001$ in both lines). Combination treatment with 5-FU further amplified

the γ-H2AX signal (HCT116: 5.1 ± 0.7-fold; LoVo: 4.6 ± 0.8-fold vs. control, $p<0.001$), consistent with enhanced DNA damage checkpoint activation when both agents are combined. All band intensities were normalized to GAPDH loading controls and quantified using ImageJ software (Figure 5).

We note that the temporal relationship between γ-H2AX induction and activation of apoptotic markers was not systematically evaluated in this study. The observed γ-H2AX elevation may therefore reflect either direct induction of DNA double-strand breaks by linarin or secondary nuclear fragmentation during the apoptotic cascade. Future time-course experiments measuring γ-H2AX at early time points (6, 12, and 24 hours) before full apoptotic commitment will be required to distinguish among these mechanistic possibilities. The data as presented are accordingly described as consistent with enhanced DNA damage checkpoint signaling rather than as definitive evidence of direct DNA strand break induction.

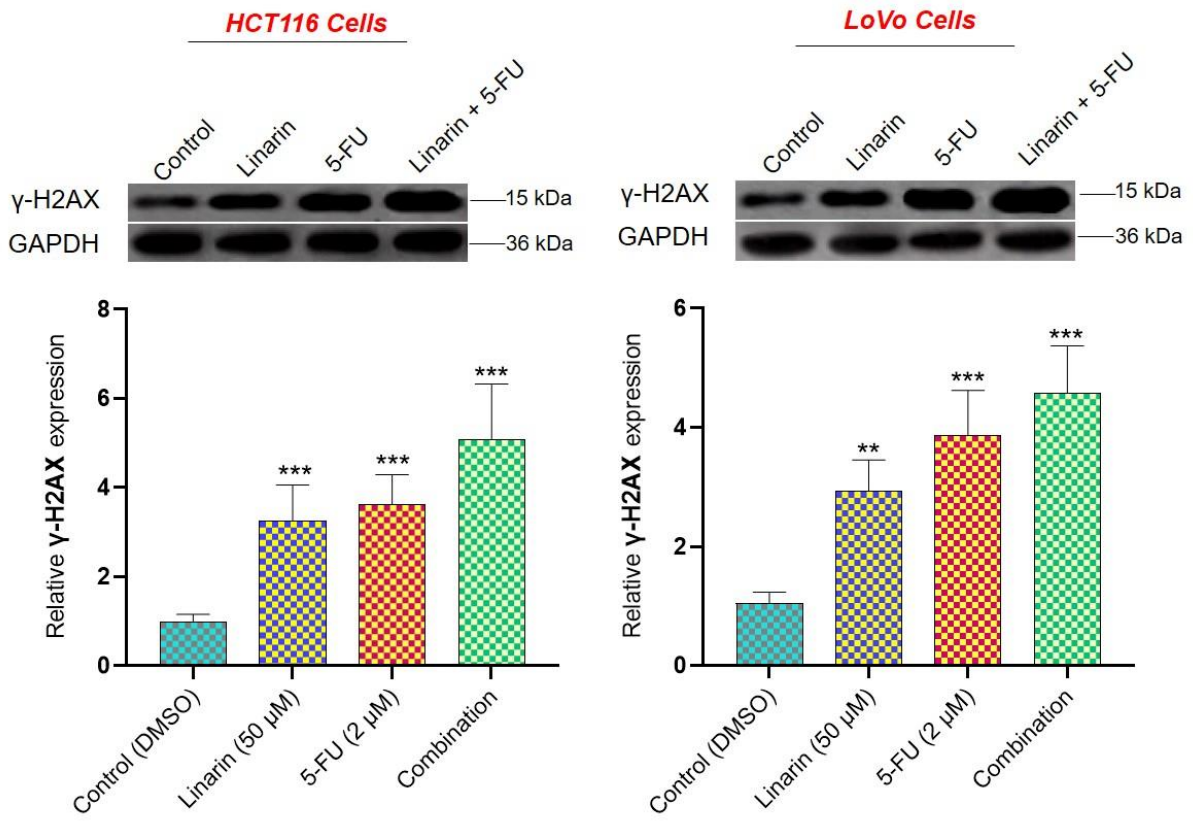

Figure 5. Linarin induces a DNA damage response. Western blot analysis of γ-H2AX (Ser139) expression in HCT116 and LoVo cells following treatment with linarin (50 μM), 5-FU (2 μM), or their combination for 48 hours. GAPDH serves as a loading control. Band intensities normalized to GAPDH and quantified by ImageJ: HCT116 — linarin: 3.2 ± 0.4-fold, combination: 5.1 ± 0.7-fold; LoVo — linarin: 2.9 ± 0.5-fold, combination: 4.6 ± 0.8-fold vs. control (all $p<0.001$). Data represent mean ± SD from three independent biological replicates (n = 3), each with technical triplicates. **5-FU:** 5-fluorouracil; **SD:** Standard deviation; **GAPDH:** Glyceraldehyde 3-phosphate dehydrogenase; **μM:** Micromolar; **γ-H2AX:** H2AX phosphorylated at Serine 139.

Discussion

The present study provides mechanistic proof-of-concept that linarin, a naturally occurring flavone glycoside, exhibits anticancer activity against colorectal cancer cells and enhances sensitivity to 5-FU by engaging the p53/p21 tumor suppressor pathway. Our findings reveal a mechanistic framework by which a flavone glycoside

can potentiate chemosensitivity by reactivating the p53 pathway, with important implications for the rational design of combination strategies in colorectal cancer. We wish to be explicit at the outset of this Discussion that the present study is scoped as an in vitro mechanistic proof-of-concept investigation. The experimental dataset, while internally consistent and functionally validated, carries defined limitations — principally the use of an intrinsic rather than acquired resistance model, incomplete upstream mechanistic characterization, the absence of flow cytometric apoptosis quantification, and the pharmacological gap between in vitro effective concentrations and estimated achievable systemic concentrations — that are each addressed below with explicit prioritization of the corresponding future experiments.

Our cytotoxicity screening revealed that linarin exhibits dose-dependent antiproliferative effects with IC_{50} values ranging from 122.8 to 210.2 μM at 48 hours. We acknowledge that these concentrations substantially exceed estimated achievable plasma concentrations of unmodified linarin following oral administration, and that this represents a fundamental pharmacological challenge for translational development. In the broader flavonoid literature, many naturally occurring flavone glycosides — including quercetin, luteolin, and acacetin — exhibit comparable in vitro IC_{50} values in the 100–300 μM range, while retaining translational interest when delivery is optimized. Published nanoformulation strategies, including poly(lactic-co-glycolic acid) (PLGA) nanoparticle encapsulation, liposomal delivery systems, and chitosan-based nanocarriers, have achieved two- to tenfold reductions in effective in vitro concentration for structurally related flavone glycosides and substantially improved bioavailability parameters in rodent pharmacokinetic studies. Prodrug conversion to the more membrane-permeable acacetin aglycone, which is the predominant metabolic product of linarin following intestinal β-glucosidase activity, may further reduce the effective concentration requirement.

Furthermore, the combination strategy reported in the present study — in which co-administration of linarin at 50 μM reduces the 5-FU IC_{50} by up to 70% — meaningfully distributes the effective concentration burden and provides a pharmacologically more realistic framework for clinical translation than monotherapy. Pharmaceutical formulation optimization studies, including PLGA nanoencapsulation and liposomal delivery, are explicitly designated as an essential component of the next translational phase, and in vitro-to-in vivo concentration translation modeling incorporating protein binding, gut metabolism, and tissue accumulation kinetics will be required before any clinical dose projection can be made. These in vitro findings are therefore presented strictly as mechanistic evidence and do not constitute a basis for direct clinical dose projection.

Mechanistically, linarin's profile is distinct from that of structurally related and functionally analogous flavonoids previously investigated as CRC chemosensitizers. Quercetin and apigenin primarily sensitize CRC cells through reactive oxygen species generation and mitochondrial pathway activation, with p53 involvement that is largely secondary and cell line-dependent. Acacetin — the aglycone of linarin — shows distinct selectivity profiles and weaker induction of p53 transcriptional targets in available comparative studies, with structure-activity relationship analyses suggesting that the glucose moiety in linarin influences both target selectivity and the magnitude of downstream signaling responses.[14] β-Elemene, a sesquiterpene natural product, reverses resistance in p53-deficient cells through pro-death autophagy and cyclin D3-dependent cell cycle arrest — a mechanism entirely distinct from linarin's p53-dependent transcriptional reactivation strategy.[15] The present data therefore identify linarin as occupying a mechanistically distinct niche among natural chemosensitizers,

characterized by its capacity to simultaneously stabilize p53 through post-translational modification and suppress MDM2 transcription, thereby reinforcing p53 pathway activity through complementary mechanisms.

The observation that HCT116 p53-null cells showed reduced sensitivity to linarin compared with their wild-type counterparts, and that SW480 cells harboring a gain-of-function p53 mutant showed intermediate sensitivity, together formed a p53 status-dependent gradient consistent with p53-dependent modulation of cytotoxicity. The residual cytotoxicity in p53-null cells indicates that p53-independent mechanisms also contribute at the concentrations employed. At concentrations exceeding 100 μM, flavone glycosides may exhibit pro-oxidant effects, potentially generating reactive oxygen species that trigger mitochondrial membrane permeabilization and caspase activation via p53-independent pathways. Comprehensive ROS measurement using DCFH-DA fluorescence assays, mitochondrial membrane potential assessment by JC-1 staining, and N-acetylcysteine rescue experiments represent important future experiments to determine the relative contributions of p53-dependent and ROS-mediated mechanisms, particularly at higher concentrations. This mechanistic complexity is explicitly acknowledged as a boundary condition of the p53-pathway-specific conclusions drawn in this study.

The current study employed LoVo cells as a model of intrinsic 5-FU resistance, a choice grounded in the well-documented p53 pathway dysfunction in this line and in the established literature demonstrating that wild-type p53 restores 5-FU sensitivity in LoVo-derived sublines.[12] We wish to be transparent; however, that intrinsic resistance, as modeled by LoVo cells, does not recapitulate the molecular complexity of acquired chemoresistance, which involves progressive selection for resistance-conferring alterations, including thymidylate synthase upregulation, DPD overexpression, multidrug resistance protein overexpression, and dynamic epigenetic reprogramming. The generation of stable acquired 5-FU-resistant CRC sublines by chronic drug exposure — followed by full molecular characterization of resistance mechanisms and evaluation of linarin's capacity to modulate them — is designated as the primary experimental priority in the next phase of this research program. Until this work is completed, the chemosensitization effects reported in the present study should be interpreted within the specific context of intrinsic p53-related resistance rather than as evidence of broad-spectrum acquired chemoresistance reversal.

The clinical significance of p53 status in 5-FU sensitivity has been extensively documented. Recent chromatin accessibility studies have shown that p53 expression confers sensitivity to 5-FU by regulating chromatin dynamics, with 5-FU-accessible chromatin regions primarily associated with genes involved in cell death pathways.[16] Our findings complement these epigenetic studies by demonstrating that pharmacological reactivation of the p53 pathway with a natural compound can enhance 5-FU-mediated cytotoxicity. The combination indices ranging from 0.52 to 0.88 in p53-proficient lines, confirmed by isobologram analysis, indicate synergism, with the most pronounced sensitization observed in intrinsically chemoresistant LoVo cells. The near-additive CI in p53-null cells (0.77) and intermediate synergy in SW480 cells (0.53) further reinforce the p53-dependent nature of the synergistic interaction.

Our mechanistic investigations revealed that linarin promotes p53 stabilization by enhancing phosphorylation at Ser15 and Ser20, critical sites for p53 transcriptional activity and implicated in chemosensitization across various cancer types. We acknowledge that the precise upstream mechanism by which linarin promotes these phosphorylation events remains incompletely characterized. The central unresolved question is whether linarin activates the ATM and/or ATR kinase cascade—the primary mediators of DNA damage-induced p53

stabilization—or whether it operates through alternative upstream mechanisms, such as inhibition of protein phosphatase activity, modulation of the ubiquitin-proteasome system, or direct disruption of the MDM2–p53 interaction. Resolution of this question will require: (i) ATM and ATR kinase activity assays, including phosphorylation of established ATM substrates such as CHK2 (Thr68) and ATR substrates such as CHK1 (Ser317); (ii) p53-responsive luciferase reporter assays using constructs driven by p53-response element-containing promoters (such as PG13-Luc), which would provide direct quantitative evidence of enhanced p53 transcriptional activity independent of protein level changes; and (iii) co-immunoprecipitation assays to determine whether linarin physically disrupts the MDM2–p53 interaction, which would provide mechanistic evidence for an upstream stabilization mechanism. These experiments are designated as the highest-priority mechanistic studies in the follow-up investigation.

The concurrent suppression of MDM2 at both the mRNA and protein levels is particularly significant, as MDM2 overexpression is a major mechanism of p53 inactivation in cancers that retain wild-type p53. The parallel reduction at both transcript and protein levels strongly implicates transcriptional repression as the primary mechanism of MDM2 downregulation. Interestingly, 5-FU has been shown to paradoxically promote stemness in CRC through p53-mediated activation of the WNT/β-catenin pathway,[17] raising the possibility that the balance between p53's pro-apoptotic and pro-survival transcriptional outputs may be context-dependent. Our findings indicate that linarin-mediated p53 activation in combination settings primarily promotes pro-apoptotic rather than pro-stemness programs, potentially because concurrent MDM2 suppression shifts the p53 transcriptional balance toward apoptotic target genes.

The significant upregulation of p21 (5.4-fold in HCT116 cells and 4.7-fold in LoVo cells) is a critical mechanistic component. p21 functions as a cyclin-dependent kinase inhibitor that enforces cell cycle arrest at G1/S and G2/M checkpoints, and its role in chemosensitization has been well documented. Given the magnitude of the observed p21 induction, G1/S checkpoint activation is strongly predicted and consistent with established p21 biology. We acknowledge, however, that direct flow cytometric cell cycle analysis was not performed in the current study, which represents a gap in the mechanistic evidence for p21's cytostatic role. Quantitative cell cycle distribution analysis by propidium iodide staining and flow cytometry — specifically to confirm G1/S accumulation in linarin-treated cells and its abrogation following p21 siRNA knockdown — is designated as a high-priority experiment in the follow-up investigation, alongside Annexin V/PI apoptosis quantification.

Regarding the broader characterization of apoptosis, we wish to be explicit that the current dataset provides convergent biochemical evidence from two independent assays — an internucleosomal DNA fragmentation ELISA and a caspase-3/PARP Western blot analysis — consistent with caspase-dependent programmed cell death. The cell-line-specific pattern of apoptotic induction, which is attenuated in p53-null cells and intermediate in LoVo cells, is internally consistent with the mechanistic model and viability data throughout the manuscript. We acknowledge, however, that definitive quantification of apoptotic, necrotic, and viable populations requires Annexin V/PI flow cytometry, which was not performed due to constraints on instrument availability during the study period. We further acknowledge that contributions of necroptosis, ferroptosis, and autophagic cell death have not been excluded. Annexin V/PI flow cytometric validation, combined with inhibitor-based exclusion of non-apoptotic death modalities, will be essential components of the follow-up experimental program.

Our investigation of DNA damage markers revealed significant increases in γ-H2AX (Ser139) expression, consistent with DNA double-strand break signaling. This finding aligns with p53's established role in coordinating DNA damage responses and is consistent with prior reports that natural compounds can amplify 5-FU-induced DNA damage by engaging the p53 pathway.[15] The enhanced γ-H2AX signal observed in combination treatments suggests that linarin sensitizes cells to 5-FU-induced DNA damage through multiple complementary mechanisms. However, as noted in the Results section, the precise contribution of direct DNA strand break induction versus secondary nuclear fragmentation during apoptosis requires time-course mechanistic dissection.

Importantly, our study demonstrated favorable selectivity indices (approximately 2.0–3.3) compared to normal colonic epithelial cells, suggesting a therapeutic window that could minimize toxicity to healthy tissues. We acknowledge that NCM460 cells are immortalized and may not fully recapitulate the drug sensitivity profiles of primary intestinal epithelial cells. Future safety profiling using patient-derived normal colonic organoids will provide a more rigorous assessment of linarin's safety margin.

Taken collectively, the identified experimental priorities for the next phase of investigation are: (1) development and evaluation of acquired 5-FU-resistant CRC sublines with full resistance marker characterisation; (2) ATM/ATR kinase activation studies and p53-responsive luciferase reporter assays to characterise the upstream mechanism of p53 stabilisation; (3) MDM2–p53 co-immunoprecipitation to evaluate the physical interaction; (4) Annexin V/PI flow cytometric quantification of apoptotic populations and cell cycle distribution analysis; (5) time-course γ-H2AX studies to distinguish primary DNA damage from secondary nuclear fragmentation; (6) ROS measurement and mitochondrial membrane potential assays to characterise p53-independent death mechanisms; and (7) pharmaceutical formulation optimisation including nanoencapsulation strategies, followed by in vivo pharmacokinetic and efficacy studies in CRC xenograft models. We are committed to pursuing this experimental program and to reporting results in subsequent publications.

Future investigations should also prioritize validation in patient-derived xenograft models representing diverse CRC molecular subtypes, including consensus molecular subtypes 1 through 4. Investigation of linarin's effects in three-dimensional organoid models would inform combination strategies and reveal potential microenvironmental interactions not captured in monolayer culture. Structure-activity relationship studies comparing linarin with related flavone glycosides and structurally optimized derivatives could identify more potent analogs with improved pharmaceutical properties and reduced effective concentrations.

Conclusions

In conclusion, this study demonstrates that linarin exhibits selective cytotoxicity against p53-competent CRC cells, synergistically enhances 5-FU efficacy in a p53-dependent manner, and activates the p53/p21 tumor suppressor axis through post-translational stabilization of p53, transcriptional suppression of MDM2, and downstream induction of p21. The selectivity index of approximately 2.0–3.3 relative to normal colonic epithelium and CI values of 0.52–0.88 in p53-proficient lines provide quantitative evidence for the therapeutic rationale of a linarin/5-FU combination strategy. Loss-of-function studies using siRNA knockdown and pharmacological inhibition with pifithrin-α and UC2288 confirm the centrality of the p53/p21 axis in mediating linarin's sensitizing effects through two independent and convergent experimental strategies.

These findings are explicitly presented as mechanistic proof-of-concept evidence within a defined in vitro experimental scope. The principal limitations — use of intrinsic rather than acquired resistance models, incomplete upstream kinase characterization, absence of flow cytometric apoptosis and cell cycle quantification, and the pharmacological gap between in vitro effective concentrations and estimated achievable systemic concentrations — are acknowledged transparently, and each corresponds to a designated priority experiment in the next phase of investigation. The authors are committed to addressing these limitations systematically in the continuation of this research program.

Given the p53-dependent nature of linarin's sensitizing effects, future clinical development should prioritize CRC patients with p53-competent tumors, as identified by standard molecular profiling. These findings provide a mechanistic rationale for advancing linarin into formulation optimization studies and preclinical in vivo evaluation as an adjuvant to enhance 5-FU responsiveness in appropriately selected colorectal cancer patients.

Acknowledgments

This paper is the outcome of the Ph.D. clinical biochemistry thesis (Thesis no. 72262) approved by Tabriz University of Medical Sciences. The authors would also like to thank Shohada Clinical Research Development Unit, Shohada Hospital, Tabriz University of Medical Science, Tabriz, Iran.

Authors' Contribution

Conceptualization: Mohammad Rahmati-Yamchi, Alireza Ali Hemmati, Bahman Yousefi.
Data curation: Amir Valizadeh.
Formal analysis: Amir Valizadeh, Mohammad Ebrahimnezhad, Mehran Molavand.
Funding acquisition: Amir Valizadeh.
Investigation: Amir Valizadeh, Mohammad Ebrahimnezhad, Mehran Molavand.
Methodology: Amir Valizadeh.
Project administration: Bahman Yousefi.
Resources: Amir Valizadeh.
Software: Mehran Molavand.
Supervision: Mohammad Rahmati-Yamchi, Bahman Yousefi.
Validation: Mohammad Rahmati-Yamchi, Alireza Ali Hemmati.
Visualization: Ali Yousefzadeh, Mehran Molavand.
Writing – original draft: Amir Valizadeh, Mohammad Ebrahimnezhad, Ali Yousefzadeh, Mehran Molavand.
Writing–review & editing: Mohammad Rahmati-Yamchi, Alireza Ali Hemmati, Bahman Yousefi.

Competing Interests

The authors declare that they have no known competing financial interests or personal relationships that could have influenced the work reported in this paper.

Data Availability Statement

All data supporting our findings in this study are available from the corresponding authors upon reasonable request.

Ethical Approval

All experimental procedures were conducted in accordance with the Declaration of Helsinki and were approved by the Ethics Committee of Tabriz University of Medical Sciences (IR.TBZMED.AEC.1402.085). This study involved exclusively in vitro experimentation using established cell lines; no animal or human subjects were directly involved.

Funding

This paper is the outcome of the Ph.D. clinical biochemistry thesis (Thesis no. 72262) approved by Tabriz University of Medical Sciences.

Supplementary Files

Supplementary File 1 contains Figures S1 and S2 and Table S1.

References

1. Roshandel G, Ghasemi-Kebria F, Malekzadeh R. Colorectal Cancer: Epidemiology, Risk Factors, and Prevention. *Cancers (Basel)* 2024;16(8). doi: 10.3390/cancers16081530
2. Matsuda T, Fujimoto A, Igarashi Y. Colorectal Cancer: Epidemiology, Risk Factors, and Public Health Strategies. *Digestion* 2025;106(2):91-9. doi: 10.1159/000543921
3. Ghafouri-Fard S, Abak A, Tondro Anamag F, Shoorei H, Fattahi F, Javadinia SA, et al. 5-Fluorouracil: A Narrative Review on the Role of Regulatory Mechanisms in Driving Resistance to This Chemotherapeutic Agent. *Front Oncol* 2021;11(658636. doi: 10.3389/fonc.2021.658636
4. Sharma A, Chorawala MR, Rawal RM, Shrivastava N. Integrated blood and organ profile analysis to evaluate ameliorative effects of kaempferol on 5-fluorouracil-induced toxicity. *Scientific Reports* 2024;14(1):2363. doi: 10.1038/s41598-024-52915-6
5. Blondy S, David V, Verdier M, Mathonnet M, Perraud A, Christou N. 5-Fluorouracil resistance mechanisms in colorectal cancer: From classical pathways to promising processes. *Cancer Sci* 2020;111(9):3142-54. doi: 10.1111/cas.14532
6. Latchman J, Guastella A, Tofthagen C. 5-Fluorouracil toxicity and dihydropyrimidine dehydrogenase enzyme: implications for practice. *Clin J Oncol Nurs* 2014;18(5):581-5. doi: 10.1188/14.cjon.581-585
7. Liebl MC, Hofmann TG. The Role of p53 Signaling in Colorectal Cancer. *Cancers (Basel)* 2021;13(9). doi: 10.3390/cancers13092125
8. Sethy C, Kundu CN. 5-Fluorouracil (5-FU) resistance and the new strategy to enhance the sensitivity against cancer: Implication of DNA repair inhibition. *Biomed Pharmacother* 2021;137(111285. doi: 10.1016/j.biopha.2021.111285
9. Batra P, Sharma AK. Anti-cancer potential of flavonoids: recent trends and future perspectives. *3 Biotech* 2013;3(6):439-59. doi: 10.1007/s13205-013-0117-5
10. Mottaghipisheh J, Taghrir H, Boveiri Dehsheikh A, Zomorodian K, Irajie C, Mahmoodi Sourestani M, et al. Linarin, a Glycosylated Flavonoid, with Potential Therapeutic Attributes: A Comprehensive Review. *Pharmaceuticals (Basel)* 2021;14(11). doi: 10.3390/ph14111104

11. Kim B, Lee JH, Seo MJ, Eom SH, Kim W. Linarin down-regulates phagocytosis, pro-inflammatory cytokine production, and activation marker expression in RAW264.7 macrophages. *Food Sci Biotechnol* 2016;25(5):1437-42. doi: 10.1007/s10068-016-0223-3

12. Yu ZW, Zhao P, Liu M, Dong XS, Tao J, Yao XQ, et al. Reversal of 5-flouroucial resistance by adenovirus-mediated transfer of wild-type p53 gene in multidrug-resistant human colon carcinoma LoVo/5-FU cells. *World J Gastroenterol* 2004;10(13):1979-83. doi: 10.3748/wjg.v10.i13.1979

13. Chou TC. Drug combination studies and their synergy quantification using the Chou-Talalay method. *Cancer Res* 2010;70(2):440-6. doi: 10.1158/0008-5472.can-09-1947

14. Singh RP, Agrawal P, Yim D, Agarwal C, Agarwal R. Acacetin inhibits cell growth and cell cycle progression, and induces apoptosis in human prostate cancer cells: structure-activity relationship with linarin and linarin acetate. *Carcinogenesis* 2005;26(4):845-54. doi: 10.1093/carcin/bgi014

15. Zhang R, Pan T, Xiang Y, Zhang M, Feng J, Liu S, et al. β-Elemene Reverses the Resistance of p53-Deficient Colorectal Cancer Cells to 5-Fluorouracil by Inducing Pro-death Autophagy and Cyclin D3-Dependent Cycle Arrest. *Front Bioeng Biotechnol* 2020;8(378. doi: 10.3389/fbioe.2020.00378

16. Yang CM, Kang MK, Jung WJ, Joo JS, Kim YJ, Choi Y, et al. p53 expression confers sensitivity to 5-fluorouracil via distinct chromatin accessibility dynamics in human colorectal cancer. *Oncol Lett* 2021;21(3):226. doi: 10.3892/ol.2021.12487

17. Cho YH, Ro EJ, Yoon JS, Mizutani T, Kang DW, Park JC, et al. 5-FU promotes stemness of colorectal cancer via p53-mediated WNT/β-catenin pathway activation. *Nat Commun* 2020;11(1):5321. doi: 10.1038/s41467-020-19173-2